Tunneling and coupling between one-dimensional states in double quantum wires

H. Weman,* D. Y. Oberli, M.-A. Dupertuis, F. Reinhardt, A. Gustafsson,† and E. Kapon
Institute of Micro- and Opto-electronics, Department of Physics, Swiss Federal Institute of Technology, CH-1015 Lausanne, Switzerland
(Received 28 January 1998)

Evidence of tunneling and electronic coupling in a one-dimensional system is reported. This is accomplished by comparing low-temperature photoluminescence and photoluminescence excitation spectra of GaAs double quantum wires of different barrier widths with a full $4\times4\,\mathbf{k}\cdot\mathbf{p}$ calculation of coupled interband transitions. [S0163-1829(98)01228-4]

Low-dimensional quantum structures provide a unique system for studying tunneling and coupling of electronic states. The quantum confinement leads to the formation of well-defined (and often controllable) electronic states, allowing the systematic investigation of tunneling and coupling and their dependence on the structure parameters.[1] Electronically coupled quantum structures also permit the realization of superlattice states, yielding insight into electron and hole localization phenomena.[2] The high sensitivity of the features of electron coupling to external electric and magnetic fields makes such coupled systems interesting for device applications, providing means for performing electric and optical switching and modulation.[3]

Tunneling and coupling have been extensively studied in two-dimensional (2D) semiconductor quantum wells (QW's), showing a number of interesting phenomena including emission of coherent THz radiation, negative differential resistance, and intrinsic bistability.[4] The reduced dimensionality in one-dimensional (1D) semiconductor quantum wires (QWR's) is expected to modify the coupling features as compared with two- or three-dimensional structures. In particular, the mixing of the heavy-hole (hh) and light-hole (lh) states at the center of the Brillouin zone should facilitate hole tunneling in one dimension. In double-barrier QWR's, electron subband mixing has been predicted to induce unusual interference patterns and the occurrence of a critical barrier size for tunneling.[5] In contrast to tunneling between zero-dimensional quantum-dot structures, the remaining free propagation direction in wires allows tunneling between *propagating* electron states, suggesting interesting electron wave directional coupling phenomena that could be controlled by an external electric field.[6] Coupling of a large number of 1D wires in a QWR superlattice structure[7,8] could provide an interesting structure for studying the transition between 1D and 2D electronic systems.

Reports on experimental evidence for carrier tunneling in 1D semiconductors have mostly concerned electron tunneling observed in transport measurements.[9–11] The observation of coupling and tunneling effects in optical absorption and emission experiments is more challenging due to the high QWR interface quality required in this case. Recent progress in the preparation of 1D semiconductor structures has allowed the observation of the details of the 1D subband structure, including valence-band mixing effects, in optical spectra of V-groove QWR's.[12] In this Brief Report we describe direct evidence of tunneling and electronic coupling between 1D states in similar, double QWR (DQWR) structures. Our experimental results are compared with a detailed theoretical model including valence-band mixing, predicting a *simultaneous*, unforeseen coupling between resonant electron and resonant hole levels in these 1D wires.

The DQWR's were grown by low pressure (20 mbar) organometallic chemical vapor deposition on (100)-GaAs substrates patterned with 0.5-μm pitch, [011] oriented V grooves.[13] The asymmetric DQWR's incorporated two crescent-shaped GaAs wires separated by a thin $Al_{0.33}Ga_{0.67}As$ barrier (see Fig. 1). The structure consisted of a (nominally) 210-nm-thick $Al_{0.33}Ga_{0.67}As$ buffer, a 5.5-nm-thick GaAs narrow QWR (*n*-QWR), a thin $Al_{0.33}Ga_{0.67}As$ tunneling barrier, a 7.5-nm-thick GaAs wide QWR (*w*-QWR), and finally a (nominally) 210-nm-thick $Al_{0.33}Ga_{0.67}As$ layer to ensure complete planarization of the V grooves. The structures were designed such that the first (ground) electron state of the *n*-QWR is coupled resonantly with the third electron state of the *w*-QWR. Two samples differing mainly in barrier thickness, denoted as ''DQWR-4 nm'' (4-nm-thick barrier) and ''DQWR-2.6 nm'' (2.6-nm-thick barrier), were studied [thickness determined by transmission electron microscopy (TEM)]. In order to enhance the luminescence from the QWR's relative to that of the surrounding QW's, the (100) QW's were removed by etching.[14]

Photoluminescence (PL) and (linearly polarized) PL excitation (PLE) spectra of the DQWR's were measured at 10 K in a helium-flow cryostat, using the 488-nm line from an Ar^+

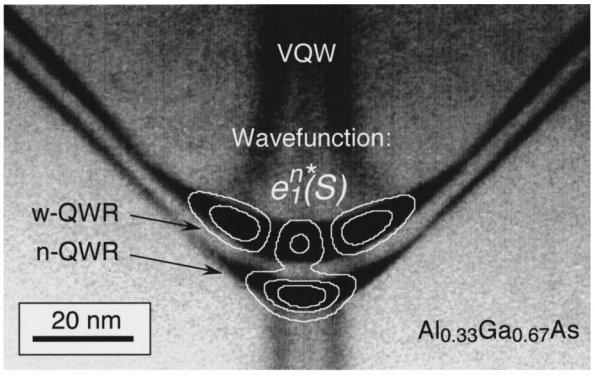

FIG. 1. Cross-sectional TEM micrograph of a 4-nm-thick barrier asymmetric GaAs double quantum wire (DQWR-4 nm) with a contour plot of the symmetric coupled electron wave function $e_1^{n*}(S)$ superimposed.

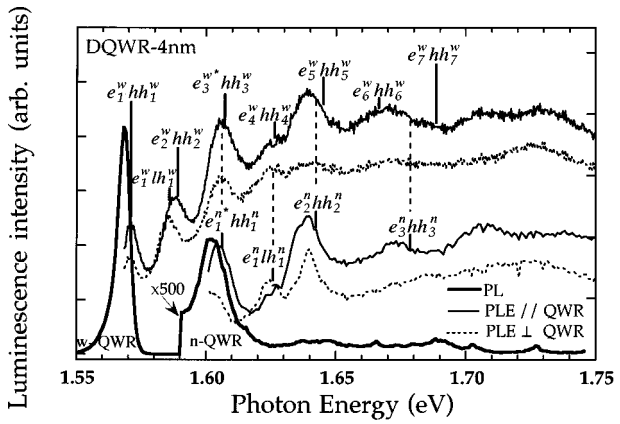

FIG. 2. Low-temperature (10 K) PL and linearly polarized PLE spectra of a 4-nm-thick barrier GaAs DQWR. Calculated energy interband transitions for the coupled DQWR are marked by solid vertical lines. The solid vertical lines are placed next to the PLE spectrum of the *w* or *n* QWR, depending on from which QWR the transitions originate. Dashed vertical lines indicate where the calculated interband transitions that originate in the *n* QWR would occur in the spectrum of the *w* QWR if tunneling is possible. The labeling of the different energy levels is explained in the text.

laser and a Ti:sapphire laser, respectively. The emitted light was dispersed through a 0.85-m double monochromator and detected with a GaAs photomultiplier. The optical power density on the sample was typically 10 W/cm^2. The polarized PLE spectra were measured with the exciting laser beam normal to the (100) surface with a linear polarization either parallel ([011] direction) or perpendicular ([011] direction) to the wire axis. Since all PLE spectra were performed on planarized samples, we avoided any polarization anisotropy caused by grating effects.

A typical dark-field cross-sectional TEM micrograph of the central part of DQWR-4 nm is shown in Fig. 1. Segregation of Ga gives rise to an $Al_xGa_{1-x}As$ vertical quantum well throughout the $Al_{0.33}Ga_{0.67}As$ barriers.[15] The *n*-QWR grown on top of the $Al_xGa_{1-x}As$ buffer has a lower self-limiting surface curvature. The lower boundary of the *w*-QWR has, however, a radius of curvature slightly larger than the self-limiting value, since here the thin $Al_xGa_{1-x}As$ barrier is not thick enough to completely re-establish the self-limiting profile.[16]

Figure 2 shows the low-temperature PL and linearly polarized PLE spectra of the DQWR-4 nm sample. The PL spectrum is dominated by an intense peak at 1.569 eV and a very weak peak at 1.602 eV. Based on PL spectra and modeling of single QWR structures of similar size and shape, we attribute these lines to exciton recombination in the *w*- and *n*-QWR's, respectively. The PL full widths at half maximum of the *w*-QWR (6 meV) and *n*-QWR (10 meV) lines are similar to those observed in single V-groove QWR's of similar sizes. The linearly polarized PLE spectra of the *n*-QWR show distinct 1D transitions and characteristic polarization anisotropy related to the 2D confinement as observed in single V-groove QWR's,[12] whereas the *w*-QWR PLE spectra are more complex due to the occurrence of tunneling, as we explain below.

In order to explore the origin of the different features in the PLE spectra, we have calculated the optical interband transitions for the coupled DQWR based on a solution of the 2D Schrödinger equation in the single-particle approximation using the full $4\times4\,\mathbf{k}\cdot\mathbf{p}$ Luttinger Hamiltonian for the valence bands. This approach has yielded an accurate determination of the electronic structure of isolated V-groove QWR's,[12] and the same material parameters are used here. The cross-sectional geometrical shapes of the QWR's were extracted from the TEM micrograph of the sample to define the potential distribution. The square of the optical matrix elements were calculated for transitions with electric fields polarized parallel and perpendicular to the wire axis. Valence-band mixing of hh and lh states in one dimension leads to ''hh-like'' and ''lh-like'' states, which we infer from the characteristics of the wave functions. The successive quantized electron and hole levels (i, j, and $k=1,2,3,...$) in the two QWR's are labeled e_i^w, hh_j^w, lh_k^w, and e_i^n, hh_j^n, lh_k^n, depending on whether the electron (e), hh-like (hh), or lh-like (lh) wave function is localized in the *w*- or *n*-QWR, respectively. An asterisk (*) indicates that the wave function is coupled, i.e., significantly distributed over the two QWR's.

The calculated interband transitions for DQWR-4 nm are indicated by vertical lines in Fig. 2, with a rigid energy redshift introduced to account for the binding energy of the exciton.[12] The PLE spectra of the *n*-QWR show clear excitonic resonances where the energy position and polarization anisotropy, especially apparent near the $e_1^n lh_1^n$ transition, are well accounted for by using the calculated interband energies and matrix elements (not shown) of the DQWR transitions that are mainly localized in the *n*-QWR. Linearly polarized PLE of the *w*-QWR also shows clear excitonic resonances, where the energy position of the six lowest resonances (below 1.68 eV) are close to the calculated DQWR transitions that are mainly localized in the *w*-QWR. However, when considering the intensity of the different transitions, one observes that the PLE signal is clearly enhanced at the energies corresponding to the $e_1^{n*} hh_1^n$ and $e_2^n hh_2^n$ transition in the *n*-QWR (see the dashed vertical lines in Fig. 2). To be noticed is the strong enhancement near the $e_3^{w*} hh_3^w$ and $e_5^w hh_5^w$ transition, whereas the $e_4^w hh_4^w$ and $e_6^w hh_6^w$ transitions are much weaker in the *w*-QWR PLE spectra. This is in very good agreement with the calculated matrix elements of the DQWR if *all optical transitions* are taken into account (whether the wave function is localized in the *w*- or *n*-QWR). These findings are direct evidence of tunneling of photoexcited carriers (electrons and/or holes) from the *n*-QWR to the *w*-QWR. Integrated PL (and PLE) intensity from the *n*-QWR is about three orders of magnitude lower than that from the *w*-QWR, indicating that the tunneling is very efficient. In order to also find evidence for strong coupling between resonant 1D states, we focus the attention on the thin barrier sample (DQWR-2.6 nm).

For DQWR-2.6 nm the tunneling transfer to the *w*-QWR is so efficient that the *n*-QWR emission is no longer observed in PL at 10 K, whereas the intensity and linewidth of the *w*-QWR line are similar to those in Fig. 2.[17] The low-temperature PLE spectra of the *w*-QWR (with excitation polarization parallel to the wire axis) in DQWR-4 nm and DQWR-2.6 nm and the calculated interband transition energies are compared in Fig. 3. The near degeneracy

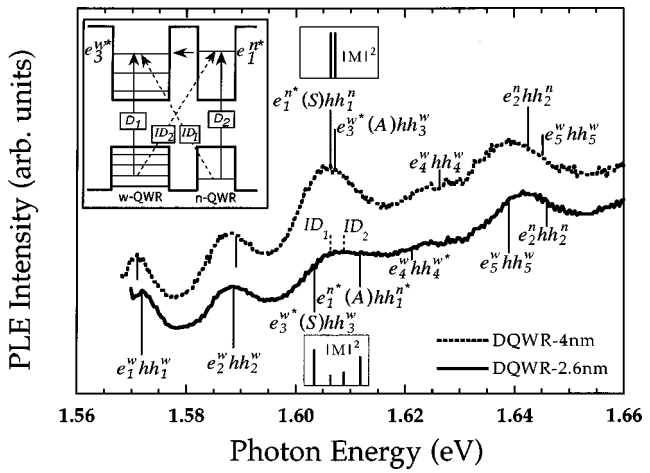

FIG. 3. Low-temperature (10 K) PLE spectra of a 2.6- (solid line) and 4-nm-thick (dashed line) barrier GaAs DQWR with the excitation polarization parallel to the wire axis. Calculated energy interband transitions for the coupled DQWR's are marked by solid vertical lines (spatially indirect transitions in DQWR-2.6 nm are marked with dashed vertical lines). The inset shows a schematic band diagram of the asymmetric DQWR. Allowed direct (D_1 and D_2), and indirect (ID_1 and ID_2), optical interband transitions are marked with solid and dashed arrows, respectively. Calculated squared optical matrix elements of the transitions involved in the coupling are shown directly below (DQWR-2.6 nm) and above (DQWR-4 nm) the PLE spectra.

between the e_3^w level in the w-QWR with the e_1^n level in the n-QWR leads to a splitting of the two electron levels into symmetric (S) and antisymmetric (A) states. Apart from the two spatially direct transitions, D_1 $[e_3^{w*}(S)hh_3^w]$ and D_2 $[e_1^{n*}(A)hh_1^{n*}]$, two spatially indirect transitions, ID_1 $[e_3^{w*}(S)hh_1^{n*}]$ and ID_2 $[e_1^{n*}(A)hh_3^w]$ are also made possible by the coupling, as shown schematically in the energy band diagram in the inset to Fig. 3. In order to compare the relative importance of the various coupled transitions in the PLE spectra, the calculated squared optical matrix elements of these transitions are shown directly below (DQWR-2.6 nm) and above (DQWR-4 nm) the PLE spectra in Fig. 3. The effect of the coupling is observable as a plateau near the original (uncoupled) $e_3^w hh_3^w$ transition in the PLE spectrum of the narrow barrier sample, presumably due to the combined absorption from the four (inhomogeneously broadened) coupled transitions (see Fig. 3). Other transitions are unaffected by the coupling. We calculate a splitting energy of 0.2 meV between the $e_1^{n*}(S)hh_1^n$ and $e_3^{w*}(A)hh_3^w$ transition for DQWR-4 nm, and 8.9 meV between the $e_3^{w*}(S)hh_3^w$ and $e_1^{n*}(A)hh_1^{n*}$ transition for DQWR-2.6 nm. For DQWR-2.6 nm we also find that apart from the coupling of electron levels e_3^{w*} and e_1^{n*}, the hole level hh_4^{w*} (66% hh like) in the w-QWR is also resonant with the hole level hh_1^{n*} (87% hh like) in the n-QWR. In principle we have thus achieved a DQWR system with a *simultaneous* resonant tunneling for the ground state holes (from hh_1^{n*} to hh_4^{w*}) and the ground state electrons (from e_1^{n*} to e_3^{w*}) from the n-QWR to the w-QWR.

We have examined the effect of wire width and barrier width nonuniformities on the DQWR coupling. The PLE spectra of Fig. 3 were intentionally measured at spatial positions where the PL peaks of the w-QWR were at the same energy on both samples (1.569 eV). We have also measured the PL and the linearly polarized PLE spectra at different locations across both DQWR samples. For DQWR-4 nm, the energy difference between the PLE peak of the n-QWR and w-QWR was found to be constant (34 ± 1 meV), and for DQWR-2.6 nm only slight variations in the shape or energy position of the plateau were observed. For both samples the lateral subband separation between the $e_1^w hh_1^w$ and $e_2^w hh_2^w$ transition in the w-QWR was found to be constant (17 ± 1 meV for DQWR-4 nm and 16 ± 1 meV for DQWR-2.6 nm), and well fitted to the calculated energy separations. Since the energy separation between the $e_1^w hh_1^w$ and $e_2^w hh_2^w$ transition is almost independent of the difference in barrier thickness and the presence of the n-QWR for our structures (only uncoupled w-QWR states involved), we conclude that the electron and hole levels in the w-QWR are accurately determined for both samples.

We also considered the possibility that the plateau in Fig. 3 is due to the misalignment of the ground state levels e_1^n and e_3^w with respect to each other in the two DQWR's. To allow for a small variation of the level alignment in our model, we have adjusted the energy position of the e_1^n level by ΔE_e by vertically shifting the bottom interface of the n-QWR for each DQWR, while keeping the e_3^w level constant. The e_1^n level can thus be shifted and tuned through the maximum coupling region. We find that the bottom interface needs to be adjusted by less than a monolayer (from the best fit of the boundaries to the TEM's) in order to reach maximum coupling. The splitting energies at maximum coupling between the symmetric and antisymmetric electron wave functions for DQWR-4 nm and DQWR-2.6 nm are calculated to be 1.4 and 4.5 meV. Coupling is achieved over less than half a monolayer thickness variation for DQWR-4 nm, and over a full monolayer thickness variation for DQWR-2.6 nm. From an analysis of the dispersion curve and the electron probability density of the fully coupled wave functions, we characterize DQWR-4 nm to be mainly in the *weak-coupling regime*, and DQWR-2.6 nm to be mainly in the *strong-coupling regime*.[18] Since our QWR's exhibit monolayer variations across the probed area, *maximum coupling* is achieved locally at numerous points along the wires for both samples. However, DQWR-2.6 nm achieves strong coupling everywhere, while DQWR-4 nm only very locally. A contour plot of the $e_1^{n*}(S)$ wave function for DQWR-4 nm at maximum coupling is superimposed on the TEM micrograph in Fig. 1.

The electron energies calculated by the best fit of the boundaries to the TEM's (Fig. 3) are within the strong-coupling regime for DQWR-2.6 nm, and within the weak-coupling regime for DQWR-4 nm. Therefore, we can infer from the calculations (1) that the observation of the PLE plateau in DQWR-2.6 nm is unambiguously an electronic coupling effect caused by the reduced barrier thickness; and (2) that no plateau is observed in the PLE of DQWR-4 nm due to the weak coupling of close to degenerate electron levels. Let us note that the results demonstrate that the hole

energies *must* be included in the splitting of the transition energies, and that the *indirect* transitions,[18] as shown in Fig. 3, also contribute.

From the previous discussion it is clear that electron level e_3^{w*} in the *w*-QWR and electron level e_1^{n*} in the *n*-QWR are close enough in energy to induce resonant tunneling. It is also very likely that the hole levels are near resonance and therefore coupled, as the calculations showed for DQWR-2.6 nm. The hole tunneling is, however, more complex than the electron tunneling due to valence-band mixing effects, and several studies have pointed out the importance of valence-band mixing for understanding the hole tunneling in two dimensions.[19–21] Roussignol *et al.* showed that a hh state in one well can elastically scatter into a lh state in the second well quite efficiently, as a consequence of the strong valence-band mixing at $k_{\|} \neq 0$.[21] Since valence-band mixing occurs already at $k_{\|}=0$ for 1D systems we believe that hole tunneling is possible between all hole levels near resonance, even at $k_{\|}=0$. Due to such *simultaneous* electron and hole coupling, we cannot rule out the possibility that it is a correlated electron-hole pair (exciton) that tunnels as a whole between the two QWR's. To investigate these interesting issues further, we are planning to perform time-resolved studies on biased DQWR's, and theoretical calculations of tunneling rates.

In summary we have investigated electronic tunneling and coupling in asymmetric double quantum wires grown on V-grooved GaAs substrates. Evidence of tunneling has been provided by low-temperature PL and PLE spectroscopy. Electronic coupling effects have been demonstrated by comparing PLE spectra for samples with different barrier widths with a full 4×4 $\mathbf{k}\cdot\mathbf{p}$ calculation of the interband transitions for the coupled DQWR. An interesting possibility of having a simultaneous tunneling between resonant 1D electron levels and resonant 1D hole levels, is also predicted by our model.

We wish to thank A. Sadeghi, A. Rudra, and L. Sagalowicz for their help in the course of this work. This work was supported by the Swiss National OPTIQUE II Priority Program and by the Fonds National Suisse de la Recherche Scientifique.

*Permanent address: Dept. of Physics, Linköping University, S-581 83 Linköping, Sweden.

†Present address: Dept. of Solid State Physics, Lund University, S-221 00 Lund, Sweden.

[1] L. L. Chang, E. E. Mendez, and C. Tejedor, *Resonant Tunneling in Semiconductors* (Plenum, New York, 1990), Vol. 277.

[2] E. E. Mendez, F. Agulló-Rueda, and J. M. Hong, Phys. Rev. Lett. **60**, 2426 (1988).

[3] D. A. B. Miller, Opt. Photonics News **1**, 7 (1990).

[4] R. Ferreira and G. Bastard, Rep. Prog. Phys. **60**, 345 (1997).

[5] A. Sa'ar, J. Feng, I. Grave, and A. Yariv, J. Appl. Phys. **72**, 3598 (1992).

[6] S. Nara, Y. Hara, Y. Nomura, and N. Tsukada, Jpn. J. Appl. Phys., Part 1 **32**, 1210 (1993).

[7] H. Weman, M. Potemski, M. E. Lazzouni, M. S. Miller, and J. L. Merz, Phys. Rev. B **53**, 6959 (1996).

[8] X.-L. Wang, M. Ogura, and H. Matsuhata, J. Cryst. Growth **171**, 341 (1997).

[9] A. Palevski, M. Heilblum, C. P. Umbach, C. M. Knoedler, A. N. Broers, and R. H. Koch, Phys. Rev. Lett. **62**, 1776 (1989).

[10] S. Tarucha, Y. Hirayama, T. Saku, and T. Kimura, Phys. Rev. B **41**, 5459 (1990).

[11] A. Zaslavsky, D. C. Tsui, M. Santos, and M. Shayegan, Appl. Phys. Lett. **58**, 1440 (1991).

[12] F. Vouilloz, D. Y. Oberli, M.-A. Dupertuis, A. Gustafsson, F. Reinhardt, and E. Kapon, Phys. Rev. Lett. **78**, 1580 (1997).

[13] A. Gustafsson, F. Reinhardt, G. Biasiol, and E. Kapon, Appl. Phys. Lett. **67**, 3673 (1995).

[14] M. Walther, E. Kapon, J. Christen, D. M. Hwang, and R. Bhat, Appl. Phys. Lett. **60**, 521 (1992).

[15] G. Biasiol, F. Reinhardt, A. Gustafsson, E. Martinet, and E. Kapon, Appl. Phys. Lett. **69**, 2710 (1996).

[16] E. Kapon, G. Biasiol, D. M. Hwang, M. Walther, and E. Colas, Solid-State Electron. **40**, 815 (1996).

[17] TEM micrographs show that the geometrical dimensions of DQWR-2.6 nm are similar (within 2–3 %) to those of DQWR-4 nm, except for the $Al_{0.33}Ga_{0.67}As$ barrier which now has a central thickness of 2.6 nm.

[18] In the strong-coupling regime, the delocalized nature of the symmetric and antisymmetric electron wave functions does not allow a sharp distinction between spatially ''direct'' and ''indirect'' transitions.

[19] R. Ferreira and G. Bastard, Europhys. Lett. **10**, 279 (1989).

[20] T. B. Norris, N. Vodjdani, B. Vinter, E. Costard, and E. Böckenhoff, Phys. Rev. B **43**, 1867 (1991).

[21] P. Roussignol, A. Vinattieri, L. Carraresi, M. Colocci, and A. Fasolino, Phys. Rev. B **44**, 8873 (1991).